Cellulases adsorb reversibly on biomass lignin

Djajadi, Demi T.; Pihlajaniemi, Ville; Rahikainen, Jenni; Kruus, Kristiina; Meyer, Anne S.

Published in:
Biotechnology and Bioengineering

Link to article, DOI:
10.1002/bit.26820

Publication date:
2018

Document Version
Peer reviewed version

Cellulases adsorb reversibly on biomass lignin

Demi T. Djajadi[1]†, Ville Pihlajaniemi[2]†, Jenni Rahikainen[2], Kristiina Kruus[2], Anne S. Meyer[1]*

Affiliations:

1: Department of Chemical and Biochemical Engineering, Søltofts Plads Building 229, Technical University of Denmark, 2800 Kongens Lyngby, Denmark.

2: VTT Technical Research Center of Finland Ltd, P.O. Box 1000, 02044 VTT, Finland.

*Corresponding author:

Anne S. Meyer

Address: Søltofts Plads Building 229, Technical University of Denmark, 2800 Kongens Lyngby, Denmark

Phone: +45-45252909

Email: asme@dtu.dk

†: Equal contribution

Short running title: Cellulases adsorb reversibly on biomass lignin

Grant numbers

0603-00522B

Abstract

Adsorption of cellulases onto lignin is considered a major factor in retarding enzymatic cellulose degradation of lignocellulosic biomass. However, the adsorption mechanisms and kinetics are not well understood for individual types of cellulases. This study examines the binding affinity, kinetics of adsorption, and competition of four monocomponent cellulases of *Trichoderma reesei* during adsorption onto lignin. *Tr*Cel7A, *Tr*Cel6A, *Tr*Cel7B and *Tr*Cel5A were radiolabeled for adsorption experiments on lignin-rich residues (LRRs) isolated from hydrothermally pretreated spruce (L-HPS) and wheat straw (L-HPWS), respectively. Based on adsorption isotherms fitted to the Langmuir model, the ranking of binding affinities was *Tr*Cel5A > *Tr*Cel6A > *Tr*Cel7B > *Tr*Cel7A on both types of LRRs. The enzymes had higher affinity to the L-HPS than to the L-HPWS. Adsorption experiments with dilution after 1 h and 24 h and kinetic modelling were performed to quantify any irreversible binding over time. Models with reversible binding parameters fitted well and can explain the results obtained. The adsorption constants obtained from the reversible models agreed with the fitted Langmuir isotherms and suggested that reversible adsorption-desorption existed at equilibrium. Competitive binding experiments showed that individual types of cellulases competed for binding sites on the lignin and the adsorption data fitted the Langmuir adsorption model. Overall, the data strongly indicate that the adsorption of cellulases onto lignin is reversible and the findings have implications for development of more efficient cellulose degrading enzymes.

Graphical Abstract

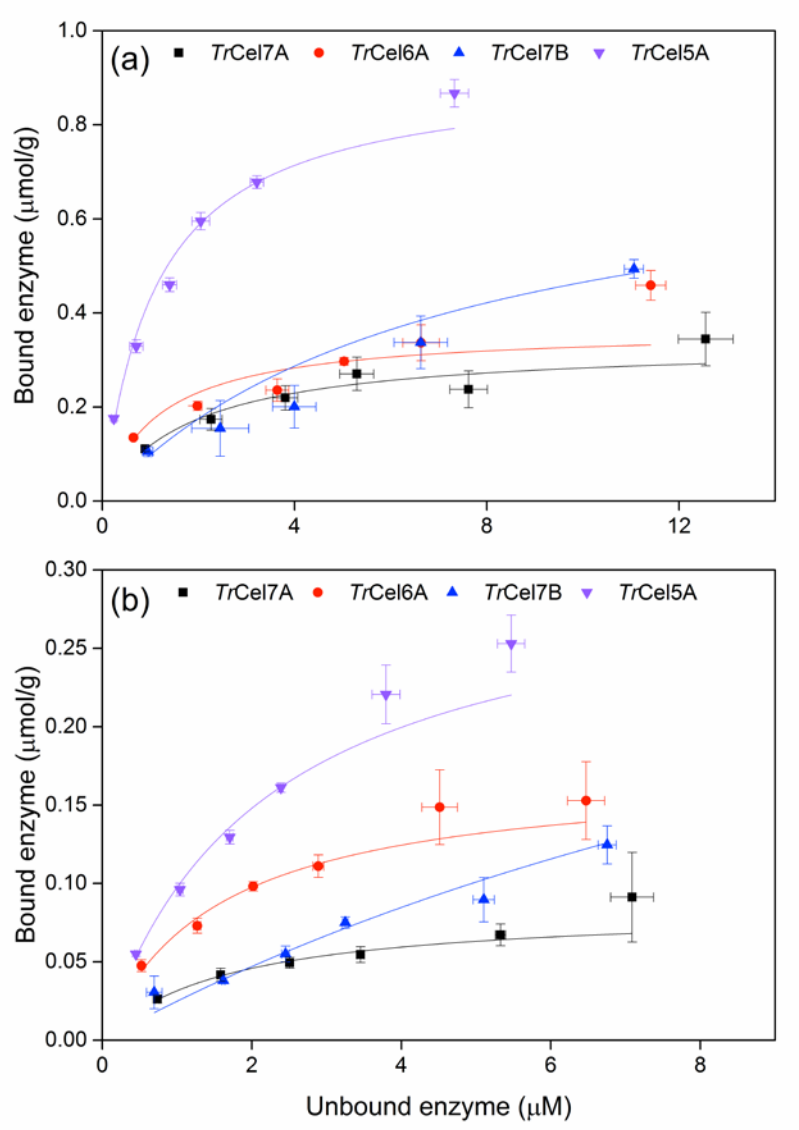

Adsorption of cellulases onto lignin is considered a major factor in retarding enzymatic cellulose degradation of lignocellulosic biomass. However, the adsorption mechanisms and kinetics are not well understood for individual types of cellulases. This study examines the binding affinity, kinetics of adsorption, and competition of four monocomponent cellulases of *Trichoderma reesei* during adsorption onto lignin.

Key words: cellulase, lignin, biomass, adsorption, reversible, competition

Introduction

Lignin has been considered as one of the major obstructions in biorefinery operations aiming at enzymatically converting cellulose in lignocellulosic biomass into glucose prior to further downstream processing (Li, Pu, & Ragauskas, 2016). Non-productive adsorption of cellulases onto lignin is considered an important mechanism behind retardation of enzymatic cellulose degradation in lignocellulose-based processes (Liu, Sun, Leu, & Chen, 2016; Saini, Patel, Adsul, & Singhania, 2016; Sipponen et al., 2017). Studies have reported adsorption of cellulases onto lignin isolated from various biomass feedstocks and have correlated such adsorption with the observed retardation of enzymatic degradation of pure model cellulose in the presence of the isolated lignin (Kellock, Rahikainen, Marjamaa, & Kruus, 2017; Rahikainen et al., 2011; Tu, Pan, & Saddler, 2009). Hydrophobic interaction (Sammond et al., 2014; Tu et al., 2009), electrostatic interaction (Lan, Lou, & Zhu, 2013; Yarbrough et al., 2015), and hydrogen bonding (Sewalt, Glasser, & Beauchemin, 1997; Yu et al., 2014) have been regarded as the cause of the non-productive binding of cellulases to lignin. However, more recently, it has been recognized that several interactions between the different chemical groups in the lignin and in the enzymes may be occurring simultaneously (Liu et al., 2016; Nakagame, Chandra, Kadla, & Saddler, 2011; Rahikainen, Evans, et al., 2013; Sipponen et al., 2017).

Accordingly, several mitigating efforts by including additives such as BSA and surfactants in the hydrolysis reaction (Börjesson, Engqvist, Sipos, & Tjerneld, 2007; Yang & Wyman, 2006), engineering the charge of the enzymes (Whitehead, Bandi, Berger, Park, & Chundawat, 2017) or changing the pH of the reaction (Lan et al., 2013) have been employed with varying degrees of success. However, the precise mechanism in the enzyme-lignin interaction that leads to reduced recoverable activity or cellulose conversion is not well understood, especially with respect to the individual types of enzymes present in a cellulolytic mixture. Several studies have indicated irreversible binding and/or reduced recovery of activity during adsorption of cellulases on isolated lignin (Kellock et al., 2017; Rahikainen et al., 2011) or during enzymatic hydrolysis of pretreated lignocellulosic biomass (Gao, Haarmeyer, Balan, Whitehead, & Dale, 2014; Várnai, Viikari, Marjamaa, & Siika-aho, 2011). Yet, there are also studies reporting that isolated lignin neither retarded the enzymatic cellulose degradation (Barsberg, Selig, & Felby, 2013; Djajadi et al., 2018) nor reduced the recoverable cellulase activity after adsorption (Rodrigues, Leitão, Moreira, Felby, & Gama, 2012). These studies suggested that the binding of the enzymes on lignin is reversible by nature. However, such a phenomenon has not been investigated up to date as the loss of enzyme activity due to non-productive adsorption onto lignin has in general been considered as irreversible (Saini et al., 2016).

Generally, adsorption of protein onto solid surfaces is known as a dynamic process involving partial exchange of adsorbed and desorbed states. During the process however, the constant conformational rearrangements between the two states can compromise the structural integrity of the protein, leading to irreversible structural change(s) that can affect subsequent adsorption behavior (Norde, 1986). This denaturation due to protein unfolding has been suggested as the cause of reduced

enzymatic cellulose degradation in the presence of lignin (Rahikainen et al., 2011; Sammond et al., 2014), especially at elevated temperature (Börjesson et al., 2007; Rahikainen et al., 2011). Consequently, cellulose hydrolysis by thermostable enzymes was affected less by lignin compared to that performed by enzymes with lesser thermostability (Rahikainen, Moilanen, et al., 2013). In this study, well-characterized monocomponent cellulases derived from *Trichoderma reesei* were studied to assess their binding affinity on lignin-rich residues from different biomass feedstocks, to distinguish reversible and irreversible bindings over extended reaction time using kinetic experiments and modelling, as well as to assess their competition with one another during adsorption on lignin.

Materials and methods

Biomass pretreatment and lignin isolation

Lignin-rich residues (LRRs) were obtained from extensive enzymatic hydrolysis of hydrothermally pretreated spruce (HPS) and wheat straw (HPWS) followed by protease treatment optimized from previous method (Rahikainen et al., 2011). The hydrothermal pretreatment (HTP) conditions were 195°C for 15 min (log R_0 = 3.97) for wheat straw (Djajadi et al., 2017) and 200°C for 10 min (log R_0 = 3.94) for spruce. The composition of the LRRs have been determined using the National Renewable Energy Laboratory (NREL) protocol (Sluiter et al., 2008). The LRRs contained 82.3% and 83.7% total lignin for lignin from hydrothermally pretreated spruce (L-HPS) and wheat straw (L-HPWS), respectively. The isolation method was shown to remove adsorbed enzymes as indicated by the reduction in nitrogen content of the LRRs (Djajadi et al., 2018; Rahikainen et al., 2011). Even though the isolated LRRs contained residual carbohydrates, the carbohydrates were not accessible to the enzymes and were not traceable to the surface of the LRRs (Djajadi et al., 2018).

Enzyme purification and characterization

Monocomponent cellulases, i.e. cellobiohydrolases (CBHs: *Tr*Cel7A and *Tr*Cel6A) and endoglucanases (EGs: *Tr*Cel7B and *Tr*Cel5A) were produced from *Trichoderma reesei* (Teleomorph *Hypocrea jecorina*) at VTT and were purified according to previous work (Suurnäkki et al., 2000). The molecular weights (M_Ws), isoelectric point (pI) and hydrophobic surface characteristics (patch score) of the enzymes have been determined previously (Kellock et al., 2017; Várnai, Siika-aho, & Viikari, 2013). The activity of *Tr*Cel7A and *Tr*Cel6A was assessed by hydrolyzing 0.1% (w/v) regenerated amorphous cellulase (RAC) as substrate using 50 mg/g dosage for 2 h at 45°C and pH 5.0. The activity of *Tr*Cel7B and *Tr*Cel5A was determined using hydroxyethylcellulose 1% (w/v) (HEC) as substrate for 2 h at 45°C and pH 5.0. The products were quantified as reducing sugars using DNS (3,5-dinitrosalicylic acid). Final protein purity and protein concentrations were determined using SDS-PAGE analysis using the Criterion Imaging System and the Detergent Compatible (DC) Protein assay (Bio-Rad Laboratories Inc., CA, USA), respectively. The monocomponent enzymes were pure as indicated by the presence of single bands (Figure S1). The details of the enzymes used in this study are presented in Table I.

Radiolabeling of the enzymes through reductive methylation

The enzymes (*Tr*Cel7A, *Tr*Cel6A, *Tr*Cel7B and *Tr*Cel5A) were radiolabeled with tritium through reductive methylation using tritiated sodium borohydride ($[^3H]NaBH_4$) and formaldehyde (CH_2O) (Means & Feeney, 1968; Tack, Dean, Eilat, Lorenz, & Schechter, 1980) with modifications according to previous works (Rahikainen, Evans, et al., 2013; Wahlström, Rahikainen, Kruus, & Suurnäkki, 2014). For the reaction, 3 mg enzyme was buffer-exchanged in 0.2 M sodium borate buffer pH 8.5 at 4°C and was incubated on ice. Formaldehyde solution (Sigma–Aldrich Co., MO, USA) was added in 5-fold molar excess of the molar concentration of free amino groups in the enzyme. $[^3H]NaBH_4$ with 100 mCi activity (5–15 Ci/mmol, PerkinElmer, MA, USA) was dissolved in 0.01 M NaOH (1 Ci/ml) and added to the reaction. After 60 min, the reaction was stopped by transferring the mixture to Econo-Pac 10 DC gel filtration column (Bio-Rad Laboratories Inc., CA, USA) and eluting it with 0.05 M sodium acetate buffer pH 5.0 to exchange the buffer solution. The protein-rich fractions were pooled and transferred to another gel filtration column. The specific radioactivities as determined by liquid scintillation counting (LSC) and protein concentration assay were 0.5, 0.5, 1.7, and 2.8 Ci/mmol for *Tr*Cel7A, *Tr*Cel6A, *Tr*Cel7B and *Tr*Cel5A respectively. Accordingly, in the subsequent adsorption experiments, the ^3H-labeled enzymes were mixed in 1:20 (for *Tr*Cel7A and *Tr*Cel6A) and 1:50 dilution ratio (for *Tr*Cel7B and *Tr*Cel5A) with their non-radiolabeled counterparts to allow accurate detection as done previously (Rahikainen, Evans, et al., 2013; Wahlström et al., 2014). SDS-PAGE analysis indicated that there was no degradation of the radiolabeled enzymes (Figure S1).

Adsorption experiments and liquid scintillation counting (LSC)

All of the enzyme adsorption experiments were performed in 0.05 M sodium acetate buffer pH 5.0 at substrate concentration of 1% DM (dry matter) and at a temperature of 45°C with moderate mixing. The temperature was chosen due to its relevance to large scale commercial applications which operate at 37-50°C (Larsen, Haven, & Thirup, 2012). After 1 h incubation, the experiment was terminated by centrifugation and the supernatant was collected for determination of unbound enzymes using LSC. The supernatant was mixed with Ultima Gold™ XR liquid scintillation cocktail (PerkinElmer, MA, USA) and the counts per minute values of the ^3H-labeled enzymes were measured using Tri-Carb 2810 TR liquid scintillation counter (PerkinElmer, MA, USA) with 15 min counting time. Enzyme blanks were used to determine the fraction of bound enzyme. Adsorption isotherms were established at an initial protein concentration range of 2-16 μM for L-HPS and 1-8 μM for L-HPWS in triplicates for each concentration. The adsorption isotherms data were fitted to the one binding-site Langmuir adsorption model (Eq. 1).

$$B = B_{max}\frac{K_{ads}[F]}{1 + K_{ads}[F]} \quad (1)$$

Where B is the amount of bound enzyme, B_{max} is the maximum adsorption capacity, K_{ads} is the Langmuir affinity constant and [F] is the concentration of unbound enzyme.

Reversibility test and kinetic modeling of adsorption

The reversibility test was conducted at similar conditions as with adsorption isotherms. The experiment was performed using *Tr*Cel5A and *Tr*Cel6A on both L-HPS and L-HPWS. The enzymes were incubated with 1% DM LRRs at concentrations of 4, 8, 16 µM for L-HPS and 2, 4, 8 µM for L-HPWS. Subsamples were taken at different time points, centrifuged, and measured to determine the amount of enzyme bound. There were two sets of reactions in which two-fold buffer dilution was performed at different time points. In the first set of reaction, the "Early Dilution", the samples were incubated for 1 h, after which a subsample was taken and dilution was performed. After dilution, the binding of the enzyme was monitored after 1, 5 and 23 h by taking subsamples. In the second set of reaction, the "Late Dilution", the samples were incubated for 24 h during which subsamples were taken after 1, 6 and 24 h incubation. After 24 h, buffer dilution was performed and subsamples were taken after 1, 5 and 23 h to follow the binding of the enzymes. The experiments were done in duplicates and enzyme blanks were used to determine the amount of the enzyme bound.

Kinetic modelling was performed by using Matlab R2015a (The Mathworks Inc., MA, USA). The differential equations of a kinetic model were solved by numerical integration using *ode15s* ordinary differential equation solver. The resulting time curves were simultaneously fitted to the combined data from the Early Dilution and Late Dilution experiments of an enzyme-lignin pair by nonlinear regression using *lsqcurvefit*. The fitting parameters included the rate constants of reversible adsorption k_{Rev}, desorption k_{-Rev}, and irreversible adsorption k_{Ir} and the maximum adsorption capacity of lignin, B_{max}. In order to find the global maximum for the iterative fitting procedure, the fitting was repeated with a full factorial set of initial value combinations with five different initial values (10, 1, 0.01, 0.0001 and 0) for each rate constant and two initial values for the adsorption capacity B_{max}, including the maximum observed adsorption and its double. For three rate constants and a single B_{max} this meant 250 repetitions of fitting. The identifiability of the parameters was assessed statistically according to previous work (Pihlajaniemi, Sipponen, Kallioinen, Nyyssölä, & Laakso, 2016), by determining the relative standard deviation (RSD) of each parameter from the set of best fitting parameters, including the sets with the R^2 at least 99% of the highest R^2.

Competitive binding experiment

Competitive binding experiments were performed similarly as with the adsorption isotherms experiments, except that an equimolar amount of another enzyme type was added on top of the other prior to the experiments to establish adsorption isotherms. *Tr*Cel5A and *Tr*Cel6A were chosen in this experiment, so that in one experiment a radiolabeled *Tr*Cel5A was accompanied with non-radiolabeled *Tr*Cel6A and vice

versa. The isotherms were established at the ranges of 2-16 μM for L-HPS and 1-8 μM for L-HPWS using triplicates for each concentration. Enzyme blanks were used to determine the fraction of bound enzyme.

Statistical analysis

One-way analysis of variance (ANOVA) was performed using JMP 12 (SAS Institute Inc., NC, USA) with post hoc analysis using Tukey–Kramer's Honestly Significant Difference (HSD) test at $p \leq 0.05$. Fitting of isotherms data to one binding-site Langmuir adsorption model was performed using OriginPro 2016 (OriginLab Corporation, MA, USA).

Results and discussion

Binding of monocomponent cellulases on lignin-rich residues

Adsorption isotherms of *Tr*Cel7A, *Tr*Cel6A, *Tr*Cel7B and *Tr*Cel5A on lignin-rich residues (LRRs) isolated from hydrothermally pretreated spruce (L-HPS) and wheat straw (L-HPWS) were established to determine their binding affinity in hydrolytic conditions (pH 5.0 and 45°C). The isotherms revealed that *Tr*Cel5A had the highest affinity on both L-HPS and L-HPWS (Figure 1). In the adsorption on L-HPS, the binding of *Tr*Cel5A was noticeably higher compared to the other enzymes, although less pronounced in the case of binding on L-HPWS. Visually, the order of the enzymes' affinity was more distinct on L-HPWS compared to L-HPS where the following order of decreasing value can be made: *Tr*Cel5A > *Tr*Cel6A > *Tr*Cel7B > *Tr*Cel7A. In general, the enzymes had higher affinity on L-HPS compared to L-HPWS as previously shown in the case of radiolabeled *Ma*Cel45A (Cel45 endoglucanase from *Melanocarpus albomyces*) (Rahikainen et al., 2013). The labeling procedure has thus been shown to work consistently despite potential modifications to the surface accessible lysine residues. Change of hydrophobicity due to methylation is minimal due to the low number of total lysine residues in the enzymes (6-13 residues). Furthermore, the procedure is known to not affect the positive charge of lysine residues (Tack et al., 1980), making it unlikely for the pI of the protein to be modified as to affect adsorption.

One binding-site Langmuir adsorption model was fitted to the isotherms data to provide quantitative parameters of the binding. The Langmuir adsorption model has previously been used to model the binding of cellulases to lignin (Börjesson et al., 2007; Rahikainen, Evans, et al., 2013; Tu et al., 2009) due to its simplicity and versatility despite the inadequacy and shortcomings to depict the adsorption of proteins on solid surface (Latour, 2015; Rabe, Verdes, & Seeger, 2011). The relative association constant (α) in particular has been shown to reflect the relative affinity during the initial slope of the isotherm (Gilkes et al., 1992; Nidetzky, Steiner, Hayn, & Claeyssens, 1994; Rahikainen, Evans, et al., 2013). Accordingly, the order of affinity based on α values (Table 2) fits with the visual observation noticed in the isotherms curve for both L-HPS and L-HPWS (Figure 1) and confirmed the previously mentioned ranking of binding affinity: *Tr*Cel5A > *Tr*Cel6A > *Tr*Cel7B > *Tr*Cel7A.

Alternatively, analyzing adsorption at the lower concentration range of an isotherm also provides information on the affinity of the enzyme in non-saturated conditions. At low initial protein concentration, the ratio of unbound compared to bound enzyme is very low. Therefore the fraction of the bound enzyme reflects the initial affinity towards the substrate without oversaturation of the surface of the adsorbent or excessive interaction among adsorbate molecules. The fraction of bound enzyme at initial protein concentration of 2 μM after 1 h showed that *Tr*Cel5A had the highest binding with 88 and 55 % of enzymes adsorbed on both L-HPS and L-HPWS, respectively (Figure 2). The degree of binding affinity based on the fraction of bound enzyme both on L-HPS and L-HPWS (Figure 2) was: *Tr*Cel5A > *Tr*Cel6A > *Tr*Cel7A = *Tr*Cel7B. To a certain extent, this also confirmed the similar previously established order based on visual observation of the isotherms curve (Figure 1) and fitted α values (Table II).

The results in this work evidently showed that *Tr*Cel5A had the highest binding affinity compared to all the tested enzymes, both in L-HPS and L-HPWS (Figures 1 and 2). In a recent study where the same set of enzymes were subjected to binding with model surface lignin isolated from HPS and HPWS on quartz crystal microbalance with dissipation monitoring (QCM-D), *Tr*Cel7B had the highest binding (Kellock et al., 2017). The finding is in contrast with this study where *Tr*Cel7B had the second lowest affinity (Table II). However, based on maximum adsorption capacity (B_{max}), the values of *Tr*Cel7B and *Tr*Cel5A were in the same magnitude both in L-HPS and L-HPWS (Table II) which can explain the discrepancy of the finding in the two works. Regardless, direct comparison between the previous QCM-D work (Kellock et al., 2017) and this current work will be difficult due to different underlying mechanisms in the methods and even properties of the isolated lignin (Rahikainen, Martin-Sampedro, et al., 2013). Both current work (Figures 1 and 2, Table II) and previous study (Kellock et al., 2017) nevertheless agreed that *Tr*Cel6A had the second highest affinity and *Tr*Cel7A had the lowest affinity from the four tested enzymes.

The binding affinity of the enzymes was compared with their intrinsic properties in order to find correlation between the two. *Tr*Cel5A, which bound the highest, has the lowest molecular weight (M_W) of the tested monocomponent cellulases (Table I). However, the trend is not consistent across the enzymes since *Tr*Cel7A, which had the lowest affinity, had the second highest M_W. The highest affinity of *Tr*Cel5A and *Tr*Cel6A correlated to their pI values, which are above the experimental pH value of 5.0. This rendered them to be positively charged and therefore increased the tendency to bind to isolated lignin-rich residues from hydrothermally pretreated spruce and wheat straw which were previously found to be negatively-charged in the experimental pH (Rahikainen, Evans, et al., 2013). However, the trend is not consistent since the pI value of the dominant band was lower in *Tr*Cel5A compared to *Tr*Cel6A (Table I). Estimated hydrophobic patch score did not provide a clear trend either since both the overall and carbohydrate binding module (CBM) scores were both second highest in the case of *Tr*Cel7A (Table I), which had the lowest affinity (Figure 1). At this point, correlating the affinity of the enzymes with their properties was not feasible, yet the enzymes displayed similar ranking of affinity in the two

substrates. Experiments at longer duration will be needed to assess the nature of the binding.

Reversibility test and kinetic modeling of adsorption

Kinetic modelling was applied for studying the proportions and potential mechanisms of reversible and irreversible adsorption of *Tr*Cel6A and *Tr*Cel5A on L-HPS and L-HPWS. First, the time course of adsorption and subsequent desorption after dilution of the system by a factor of two were determined. The dilution was performed either after 1 h (early dilution) or 24 h of adsorption (late dilution). Three initial enzyme concentrations were used, covering the linear and saturated areas of the adsorption isotherms (Figure 1). The aim was to quantify the proportion of irreversible binding from the difference in desorption after early and late dilution, and to provide data for distinguishing the different models. The idea was that the longer incubation prior to the late dilution would allow irreversible binding to advance further and lead to lower desorption of enzymes compared to the early dilution, which would allow quantification of the proportion and the rate constant of irreversible binding.

Four different kinetic models were studied. Model 1 (Eq. 2) describes reversible adsorption which may turn into irreversible by a further 1st order reaction, resulting in kinetic equations Eq. 3 and Eq. 4, where E stands for free enzymes, L for free binding sites and EL for bound enzymes, and the subscripts $_{\mathrm{Rev}}$ and $_{\mathrm{Ir}}$ refer to reversible and irreversible binding and the corresponding rate constants k. The concentration of free sites is the proportion of unoccupied sites multiplied by lignin concentration, $[\mathrm{L}] = (\mathrm{B}_{\max} - (\mathrm{EL}_{\mathrm{Rev}} + \mathrm{EL}_{\mathrm{Ir}})) * [lignin]$.

$$E + L \underset{k_{-Rev}}{\overset{k_{Rev}}{\leftrightarrow}} \mathrm{EL}_{\mathrm{Rev}} \overset{k_{Ir}}{\rightarrow} \mathrm{EL}_{\mathrm{Ir}} \qquad (2)$$

$$\frac{dEL_{Rev}}{dt} = k_{Rev}[E][L] - (k_{-Rev} + k_{Ir})[EL_{Rev}] \qquad (3)$$

$$\frac{dEL_{Ir}}{dt} = k_{Ir}[EL_{Rev}] \qquad (4)$$

Model 2 (Eq. 5) describes separate reversible and irreversible binding on the same binding sites, representing a situation where binding may occur differently, depending on e.g. orientation; therefore following the Langmuir-kinetics of reversible adsorption (Eq. 6) and a 2nd order reaction of irreversible binding (Eq. 7) in parallel.

$$E + L \underset{k_{-Rev}}{\overset{k_{Rev}}{\leftrightarrow}} \mathrm{EL_{Rev}} \qquad (5)$$
$$k_{Ir} \downarrow$$
$$\mathrm{EL_{Ir}}$$

$$\frac{dEL_{Rev}}{dt} = k_{Rev}[E][L] - k_{-Rev}[EL_{Rev}] \qquad (6)$$

$$\frac{dEL_{Ir}}{dt} = k_{Ir}[E][L] \qquad (7)$$

Models 3 and 4 represent completely reversible (Langmuirian) (Eq. 8) and completely irreversible (Eq. 9) adsorption, each follows the kinetics of Eq. 6 and Eq. 7, respectively.

$$E + L \underset{k_{-Rev}}{\overset{k_{Rev}}{\leftrightarrow}} \mathrm{EL_{Rev}} \qquad (8)$$

$$E + L_{Ir} \xrightarrow{k_{Ir}} \mathrm{EL_{Ir}} \qquad (9)$$

The models were fitted to the experimental data and compared in terms of R^2 and parameter identifiability. Identifiability describes whether the parameter value can be determined exclusively, displaying importance (or significance) of the fit, or whether it can adopt an arbitrary value, deeming it irrelevant. The identifiability was described as relative standard deviation (RSD) of each parameter at the optimum fit, determined from the set of repetitions reaching at least 99% of the best fit, according to R^2.

Majority of adsorption occurred during the first hour, after which only minor changes were observed (Figure 3); indicating that equilibrium was reached within 1 h of adsorption. *Tr*Cel6A and *Tr*Cel5A showed similar adsorption patterns, whereas they differed on L-HPS and L-HPWS (Figures S2-S5). After dilution, minor or no release of enzymes occurred from L-HPS, whereas considerable desorption from L-HPWS-lignin was observed. The lack of desorption from L-HPS appears to suggest irreversible binding, but on a closer look this conclusion turns out to be premature. In fact, completely irreversible adsorption fitted poorly to the data (Figure S6) with R^2 below 0.78 in each case (Table III). Given the high initial rate of adsorption, the long incubation should have easily allowed completion of irreversible binding, thus leading to either depletion of free enzymes or complete saturation of binding sites. However,

such behavior was not observed and instead, equilibrium was reached at each concentration between free and adsorbed enzymes and the endpoints followed a Langmuir isotherm (Figure S6). By definition, both the dynamic equilibrium and Langmuirian behavior indicate reversible adsorption.

Displaying the data from the dilution experiments as binding isotherms revealed that most of the points after dilution either fully or partially returned to the original point prior to dilution (Figures S7 and S8). In other words, the ascending isotherm (prior to dilution) overlaps with the descending isotherm (after dilution), displaying no or limited hysteresis in the adsorption. This behavior has also been described as a display of fully reversible binding during studies on the binding of monocomponent cellulases on cellulose (Palonen, Tenkanen, & Linder, 1999; Pellegrini et al., 2014). The Langmuir constants $K_{ads} = \frac{k_{Rev}}{k_{-Rev}}$ and B_{max} determined from the kinetic modelling (Table III) and those determined from the adsorption isotherms data (Table II) are found to be in agreement with one another (Figure S9). These observations further gave strong indication of reversible binding on lignin. The adsorption constant (K_{ads}) of *Tr*Cel6A and *Tr*Cel5A were lower on L-HPWS compared to L-HPS both in the adsorption isotherms fitting (Table II) and modelling data (Table III). This indicated lower binding affinity of cellulases on L-HPWS than L-HPS which is in accordance with the high desorption on L-HPWS following dilution (Figure 3). The difference in affinity can offer explanation on the previous observations where L-HPS was found to retard the enzymatic hydrolysis of model cellulose more than L-HPWS (Kellock et al., 2017; Rahikainen, Moilanen, et al., 2013).

For L-HPS, the Models 1 and 2 showed a similar fit (R^2 of 0.896–0.923) and parameter values as that of completely reversible adsorption. In contrast, poor identifiability was observed for the irreversible adsorption rate constant k_{Ir} (RSD from 140 % to 4.8×10^7 %), indicating that reversible adsorption behavior can fully explain the results. No quantifiable irreversible binding was observed and the reason for low desorption was high affinity of L-HPS (Table III). For L-HPWS, a higher amount of desorption provided a higher resolution for determining irreversible binding. Model 1 showed a slightly better fit for both enzymes (R^2 of 0.945 and 0.967) compared to reversible binding (0.936 and 0.965) with a relevant irreversible binding rate (RSD of k_{Ir} lower than that of k_{Rev} and k_{-Rev}), whereas Model 2 neither provided improvement in fit nor relevance of k_{Ir} (Table III). This suggested the possibility of partial irreversible binding on L-HPWS, i.e. the enzymes are first bound reversibly, which is then followed by further interactions leading to irreversible binding. This is in line with the idea of protein unfolding taking place after binding on lignin (Rahikainen et al., 2011; Rahikainen, Moilanen, et al., 2013; Sammond et al., 2014).

The overall good fitting ($R^2 \approx 0.9$) of the Models 1-3 nevertheless pointed out that the adsorption of monocomponent cellulases on lignin is reversible by nature, instead of being fully irreversible. The good identifiability of reversible adsorption constants, especially in Model 3 where they were better than that in Models 1 and 2, implied that the completely reversible adsorption model alone can explain the findings. Although in some ways the statement might seem contradictory to previous understanding, this

finding illustrates the need for a re-definiton of the term irreversibility and highlights that reversibility of adsorption should not be confused with binding affinity. Distinguishing between the two can be complicated, therefore, for practical purposes the activity of the enzyme during binding onto lignin should also be investigated. Loss of activity can correlate to irreversible binding, even though that does not necessarily denote a direct causal relationship. Hence this points to the need to understand the precise mechanism leading to the loss of enzyme activity. Good fitting of Model 1 in this work confirmed and expanded the nuances of the explanation of previous findings (Rahikainen et al., 2011). Initially the enzymes constantly change structural conformation as they adsorb and desorb reversibly. Incubation at elevated temperature increases the rate of the process and thus the binding affinity. As the process continues, eventually the protein structure unfolds and renders the enzymes to be bound irreversibly at a certain extent, losing activity. In future work it would be relevant to assess whether the loss of enzyme activity is aggravated at high substrate concentration (10-30% DM) due to an increased rate of adsorption, and/or whether the binding kinetics may be affected. It remains to be seen by future work whether the loss of enzyme activity and the change to irreversible binding on lignin occur sequentially, separately or simultaneously. Finally, it is important to stress that while the binding is reversible, the loss of activity due to denaturation is irreversible.

Competitive binding of cellullases

Competitive binding study was performed to find if there is competition between selected monocomponent cellulases *Tr*Cel6A and *Tr*Cel5A which had the highest binding affinity based on the adsorption isotherms (Figures 1 and 2, Table II). In this experimental setup, only the binding of radiolabeled enzyme was recorded. In the equimolar presence of one another, the enzymes showed competitive binding in the isotherms (Figure 4). The presence of *Tr*Cel6A reduced the binding of labeled *Tr*Cel5A significantly, whereas the presence of *Tr*Cel5A had less pronounced effect on the binding of labeled *Tr*Cel6A. The reduction of the binding was clearly visible in both L-HPS (Figure 4a) and L-HPWS (Figure 4b).

Fitting of one binding-site Langmuir adsorption model to the competitive adsorption isotherms still showed good fit in general (Table IV). The maximum adsorption capacity (B_{max}) of *Tr*Cel6A was less affected by *Tr*Cel5A, whereas the B_{max} of *Tr*Cel5A was reduced more significantly by *Tr*Cel6A both in L-HPS and L-HPWS (Table IV). The B_{max} values of the mixture constituted by the two enzymes were nevertheless almost similar in magnitude (Table IV). This indicated that both enzymes competed for similar binding sites and *Tr*Cel6A predominated the competitive binding albeit lower B_{max} value. Previously it was suggested that Vroman effect was present in a cellulolytic enzyme mixture where enzymes of greater affinity displaced others of lesser affinity (Yarbrough et al., 2015). In this study, affinity seemed to be not the factor since *Tr*Cel5A had higher if not similar affinity as *Tr*Cel6A based on both α and K_{ads} (Table IV). However, in the original study that coined the Vroman effect, it was shown that proteins with larger size (M_W) displaced the smaller ones (Vroman & Adams, 1969). Accordingly, *Tr*Cel6A is indeed larger than *Tr*Cel5A

(Table I), therefore suggesting size as a plausible factor that governs competitive binding.

The presence of competitive binding between two enzymes showed that monitoring the adsorption of a multi-component system such as cellulases can be difficult to perform. Nevertheless, the presence of competition and good fitting to Langmuir model also suggest that the binding of cellulases on lignin is exchangeable and thus reversible by nature. The finding thus supports the previous observations in this work and points that the binding of cellulases on lignin is both reversible and competitive as in the case of the binding of cellulases on cellulose (Kyriacou, Neufeld, & MacKenzie, 1989; Pellegrini et al., 2014).

Conclusions

The present work indicates that despite differences in the binding affinity of individual monocomponent cellulases, the binding is reversible by nature. Modelling of kinetic experiments suggests the possibility of previously reversible binding turning to irreversible which can explain the previous observations on retardation of enzymatic cellulose conversion in the presence of lignin. Due to reversible nature of binding, the negative effect of lignin can plausibly be alleviated by including additives in the reaction. Given the indication that the binding turns irreversible hence losing activity due to structural unfolding over time at elevated temperature, engineering or finding novel enzymes with improved thermostability can be an avenue to pursue. Future studies should be directed into deciphering the underlying mechanism and factors that govern the deactivation of the enzyme by lignin, especially at high substrate concentration. The competition among cellulases in the adsorption on lignin highlights the necessity to develop methods able to distinguish the binding and activity of individual enzymes in a mixture in order to identify and selectively improve the necessary enzyme component.

Nomenclature

B_{max}: maximum adsorption constant (μmol/g)

K_{ads}: Langmuir adsorption constant (l/μmol)

α: relative association constant (l/g)

E: free enzymes (μmol/l)

L: free binding sites in lignin-rich residues (g/l)

EL: bound enzymes (μmol/g)

k_{Rev}: reversible adsorption constant (l^2/μmol g h)

k_{-Rev}: reversible desorption constant (l/g h)

k_{Ir}: irreversible adsorption constant (l/g h in Model 1; otherwise l^2/μmol g h in other models)

Acknowledgments

DTD is funded by the BioValue SPIR, Strategic Platform for Innovation and Research on value added products from biomass, which is co-funded by The Innovation Fund Denmark, Case No: 0603-00522B. Miriam Kellock is thanked for preparing the L-HPS.

Statement

All authors declare no conflict of interest.

References

Barsberg, S., Selig, M. J., & Felby, C. (2013). Impact of lignins isolated from pretreated lignocelluloses on enzymatic cellulose saccharification. *Biotechnology Letters*, *35*(2), 189–195. https://doi.org/10.1007/s10529-012-1061-x

Börjesson, J., Engqvist, M., Sipos, B., & Tjerneld, F. (2007). Effect of poly(ethylene glycol) on enzymatic hydrolysis and adsorption of cellulase enzymes to pretreated lignocellulose. *Enzyme and Microbial Technology*, *41*(1–2), 186–195. https://doi.org/10.1016/j.enzmictec.2007.01.003

Djajadi, D. T., Hansen, A. R., Jensen, A., Thygesen, L. G., Pinelo, M., Meyer, A. S., & Jørgensen, H. (2017). Surface properties correlate to the digestibility of hydrothermally pretreated lignocellulosic Poaceae biomass feedstocks. *Biotechnology for Biofuels*, *10*(1), 49. https://doi.org/10.1186/s13068-017-0730-3

Djajadi, D. T., Jensen, M. M., Oliveira, M., Jensen, A., Thygesen, L. G., Pinelo, M., … Meyer, A. S. (2018). Lignin from hydrothermally pretreated grass biomass retards enzymatic cellulose degradation by acting as a physical barrier rather than by inducing nonproductive adsorption of enzymes. *Biotechnology for Biofuels*, *11*(1), 85. https://doi.org/10.1186/s13068-018-1085-0

Gao, D., Haarmeyer, C., Balan, V., Whitehead, T. a, & Dale, B. E. (2014). Lignin triggers irreversible cellulase loss during pretreated lignocellulosic biomass saccharification. *Biotechnol Biofuels*, *7*(1), 175. https://doi.org/10.1186/s13068-014-0175-x

Gilkes, N. R., Jervis, E., Henrissat, B., Tekant, B., Miller, R. C., Warren, R. A. J., & Kilburn, D. G. (1992). The adsorption of a bacterial cellulase and its two isolated domains to crystalline cellulose. *Journal of Biological Chemistry*, *267*(10), 6743–6749.

Kellock, M., Rahikainen, J., Marjamaa, K., & Kruus, K. (2017). Lignin-derived inhibition of monocomponent cellulases and a xylanase in the hydrolysis of lignocellulosics. *Bioresource Technology*, *232*, 183–191. https://doi.org/10.1016/j.biortech.2017.01.072

Kyriacou, A., Neufeld, R. J., & MacKenzie, C. R. (1989). Reversibility and competition in the adsorption of Trichoderma reesei cellulase components. *Biotechnology and Bioengineering*, *33*(5), 631–637. https://doi.org/10.1002/bit.260330517

Lan, T. Q., Lou, H., & Zhu, J. Y. (2013). Enzymatic Saccharification of Lignocelluloses Should be Conducted at Elevated pH 5.2-6.2. *Bioenergy Research*, *6*, 476–485. https://doi.org/10.1007/s12155-012-9273-4

Larsen, J., Haven, M. Ø., & Thirup, L. (2012). Inbicon makes lignocellulosic ethanol a commercial reality. *Biomass Bioenerg*, *46*, 36–45. https://doi.org/10.1016/j.biombioe.2012.03.033

Latour, R. A. (2015). The Langmuir isotherm: A commonly applied but misleading approach for the analysis of protein adsorption behavior. *Journal of Biomedical Materials Research - Part A*, *103*(3), 949–958. https://doi.org/10.1002/jbm.a.35235

Li, M., Pu, Y., & Ragauskas, A. J. (2016). Current understanding of the correlation of lignin structure with biomass recalcitrance. *Frontiers in Chemistry*, *4*, 45. https://doi.org/10.3389/fchem.2016.00045

Liu, H., Sun, J., Leu, S.-Y., & Chen, S. (2016). Toward a fundamental understanding of cellulase-lignin interactions in the whole slurry enzymatic saccharification process. *Biofuels, Bioproducts and Biorefining*, *10*, 648–663. https://doi.org/10.1002/bbb

Means, G. E., & Feeney, R. E. (1968). Reductive alkylation of amino groups in proteins. *Biochemistry*, *7*(1965), 2192–2201. https://doi.org/10.1021/bi00846a023

Nakagame, S., Chandra, R. P., Kadla, J. F., & Saddler, J. N. (2011). The isolation, characterization and effect of lignin isolated from steam pretreated Douglas-fir on the enzymatic hydrolysis of cellulose. *Bioresource Technology*, *102*(6), 4507–4517. https://doi.org/10.1016/j.biortech.2010.12.082

Nidetzky, B., Steiner, W., Hayn, M., & Claeyssens, M. (1994). Cellulose hydrolysis by the cellulases from Trichoderma reesei: a new model for synergistic interaction. *The Biochemical Journal*, *298*(1994), 705–710.

Norde, W. (1986). Adsorption of proteins from solution at the solid-liquid interface. *Advances in Colloid and Interface Science*, *25*(C), 267–340. https://doi.org/10.1016/0001-8686(86)80012-4

Palonen, H., Tenkanen, M., & Linder, M. (1999). Dynamic interaction of Trichoderma reesei cellobiohydrolases Cel6A and Cel7A and cellulose at equilibrium and during hydrolysis. *Applied and Environmental Microbiology*, *65*(12), 5229–5233.

Pellegrini, V. O. A., Lei, N., Kyasaram, M., Olsen, J. P., Badino, S. F., Windahl, M. S., … Westh, P. (2014). Reversibility of substrate adsorption for the cellulases Cel7A, Cel6A, and Cel7B from Hypocrea jecorina. *Langmuir*, *30*(42), 12602–12609. https://doi.org/10.1021/la5024423

Pihlajaniemi, V., Sipponen, M. H., Kallioinen, A., Nyyssölä, A., & Laakso, S. (2016). Rate-constraining changes in surface properties, porosity and hydrolysis kinetics of lignocellulose in the course of enzymatic saccharification. *Biotechnology for Biofuels*, *9*(1), 18. https://doi.org/10.1186/s13068-016-0431-3

Rabe, M., Verdes, D., & Seeger, S. (2011). Understanding protein adsorption phenomena at solid surfaces. *Advances in Colloid and Interface Science*, *162*(1–2), 87–106. https://doi.org/10.1016/j.cis.2010.12.007

Rahikainen, J., Evans, J. D., Mikander, S., Kalliola, A., Puranen, T., Tamminen, T., … Kruus, K. (2013). Cellulase-lignin interactions-The role of carbohydrate-binding module and pH in non-productive binding. *Enzyme and Microbial Technology*, *53*(5), 315–321. https://doi.org/10.1016/j.enzmictec.2013.07.003

Rahikainen, J., Martin-Sampedro, R., Heikkinen, H., Rovio, S., Marjamaa, K., Tamminen, T., … Kruus, K. (2013). Inhibitory effect of lignin during cellulose bioconversion: The effect of lignin chemistry on non-productive enzyme adsorption. *Bioresource Technology*, *133*, 270–278. https://doi.org/10.1016/j.biortech.2013.01.075

Rahikainen, J., Mikander, S., Marjamaa, K., Tamminen, T., Lappas, A., Viikari, L., & Kruus, K. (2011). Inhibition of enzymatic hydrolysis by residual lignins from softwood - study of enzyme binding and inactivation on lignin-rich surface. *Biotechnology and Bioengineering*, *108*(12), 2823–2834. https://doi.org/10.1002/bit.23242

Rahikainen, J., Moilanen, U., Nurmi-Rantala, S., Lappas, A., Koivula, A., Viikari, L., & Kruus, K. (2013). Effect of temperature on lignin-derived inhibition studied with three structurally different cellobiohydrolases. *Bioresource Technology*, *146*, 118–125. https://doi.org/10.1016/j.biortech.2013.07.069

Rodrigues, A. C., Leitão, A. F., Moreira, S., Felby, C., & Gama, M. (2012). Recycling of cellulases in lignocellulosic hydrolysates using alkaline elution. *Bioresource Technology*, *110*, 526–533. https://doi.org/10.1016/j.biortech.2012.01.140

Saini, J. K., Patel, A. K., Adsul, M., & Singhania, R. R. (2016). Cellulase adsorption on lignin: A roadblock for economic hydrolysis of biomass. *Renewable Energy*, *98*, 29–42. https://doi.org/10.1016/j.renene.2016.03.089

Sammond, D. W., Yarbrough, J. M., Mansfield, E., Bomble, Y. J., Hobdey, S. E., Decker, S. R., … Crowley, M. F. (2014). Predicting enzyme adsorption to lignin films by calculating enzyme surface hydrophobicity. *Journal of Biological Chemistry*, *289*(30), 20960–20969. https://doi.org/10.1074/jbc.M114.573642

Sewalt, V. J. H., Glasser, W. G., & Beauchemin, K. A. (1997). Lignin impact on fiber degradation . 3 . Reversal of inhibition of enzymatic hydrolysis by chemical modification of lignin and by additives. *Journal of Agricultural and Food Chemistry*, *45*, 1823–1828. https://doi.org/10.1021/jf9608074

Sipponen, M. H., Rahikainen, J., Leskinen, T., Pihlajaniemi, V., Mattinen, M.-L., Lange, H., … Österberg, M. (2017). Structural changes of lignin in biorefinery pretreatments and consequences to enzyme-lignin interactions - OPEN ACCESS. *Nordic Pulp and Paper Research Journal*, *32*(4), 550–571. https://doi.org/10.3183/NPPRJ-2017-32-04-p550-571

Sluiter, A., Hames, B., Ruiz, R., Scarlata, C., Sluiter, J., Templeton, D., & Crocker, D. (2008). *Determination of structural carbohydrates and lignin in biomass. Laboratory analytical procedure (LAP). NREL/TP-510-42618*. Golden, CO, USA.

Suurnäkki, A., Tenkanen, M., Siika-Aho, M., Niku-Paavola, M. L., Viikari, L., & Buchert, J. (2000). Trichoderma reesei cellulases and their core domains in the hydrolysis and modification of chemical pulp. *Cellulose*, *7*(2), 189–209. https://doi.org/10.1023/A:1009280109519

Tack, B. F., Dean, J., Eilat, D., Lorenz, P. E., & Schechter, A. N. (1980). Tritium Labeling of Proteins to High Specific Radioactivity by Reductive Methylation. *Journal of Biological Chemistry*, *255*(18), 8842–8847.

Tu, M., Pan, X., & Saddler, J. N. (2009). Adsorption of cellulase on cellulolytic enzyme lignin from lodgepole pine. *Journal of Agricultural and Food Chemistry*, *57*(17), 7771–7778. https://doi.org/10.1021/jf901031m

Várnai, A., Siika-aho, M., & Viikari, L. (2013). Carbohydrate-binding modules (CBMs) revisited : reduced amount of water counterbalances the need for CBMs. *Biotechnology for Biofuels*, *6*, 30. https://doi.org/10.1186/1754-6834-6-30

Várnai, A., Viikari, L., Marjamaa, K., & Siika-aho, M. (2011). Adsorption of monocomponent enzymes in enzyme mixture analyzed quantitatively during hydrolysis of lignocellulose substrates. *Bioresource Technology*, *102*(2), 1220–1227. https://doi.org/10.1016/j.biortech.2010.07.120

Vroman, L., & Adams, A. L. (1969). Findings with the recording ellipsometer suggesting rapid exchange of specific plasma proteins at liquid/solid interfaces. *Surface Science*, *16*, 438–446. https://doi.org/10.1016/0039-6028(69)90037-5

Wahlström, R., Rahikainen, J., Kruus, K., & Suurnäkki, A. (2014). Cellulose hydrolysis and binding with *Trichoderma reesei* Cel5A and Cel7A and their core domains in ionic liquid solutions. *Biotechnology and Bioengineering*, *111*(4), 726–733. https://doi.org/10.1002/bit.25144

Whitehead, T. A., Bandi, C. K., Berger, M., Park, J., & Chundawat, S. P. S. (2017). Negatively Supercharging Cellulases Render Them Lignin-Resistant. *ACS*

Sustainable Chemistry and Engineering, *5*(7), 6247–6252. https://doi.org/10.1021/acssuschemeng.7b01202

Yang, B., & Wyman, C. (2006). BSA treatment to enhance enzymatic hydrolysis of cellulose in lignin containing substrates. *Biotechnology and Bioengineering*, *94*(5), 611–617. https://doi.org/10.1002/bit

Yarbrough, J. M., Mittal, A., Mansfield, E., Taylor, L. E., Hobdey, S. E., Sammond, D. W., … Vinzant, T. B. (2015). New perspective on glycoside hydrolase binding to lignin from pretreated corn stover. *Biotechnology for Biofuels*, *8*(1), 214. https://doi.org/10.1186/s13068-015-0397-6

Yu, Z., Gwak, K.-S., Treasure, T., Jameel, H., Chang, H., & Park, S. (2014). Effect of lignin chemistry on the enzymatic hydrolysis of woody biomass. *ChemSusChem*, *7*, 1942–1950. https://doi.org/10.1002/cssc.201400042

Figures

Figure 1. Adsorption isotherms of radiolabeled *Tr*Cel7A, *Tr*Cel6A, *Tr*Cel7B and *Tr*Cel5A on lignin-rich residues isolated from hydrothermally pretreated (a) spruce (L-HPS) and (b) wheat straw (L-HPWS) at 45°C, pH 5.0 after 1 h. Solid lines represent fitting of the Langmuir adsorption model for one binding-site to the isotherms. Data points and error bars respectively represent average and standard deviation from three experimental replicates.

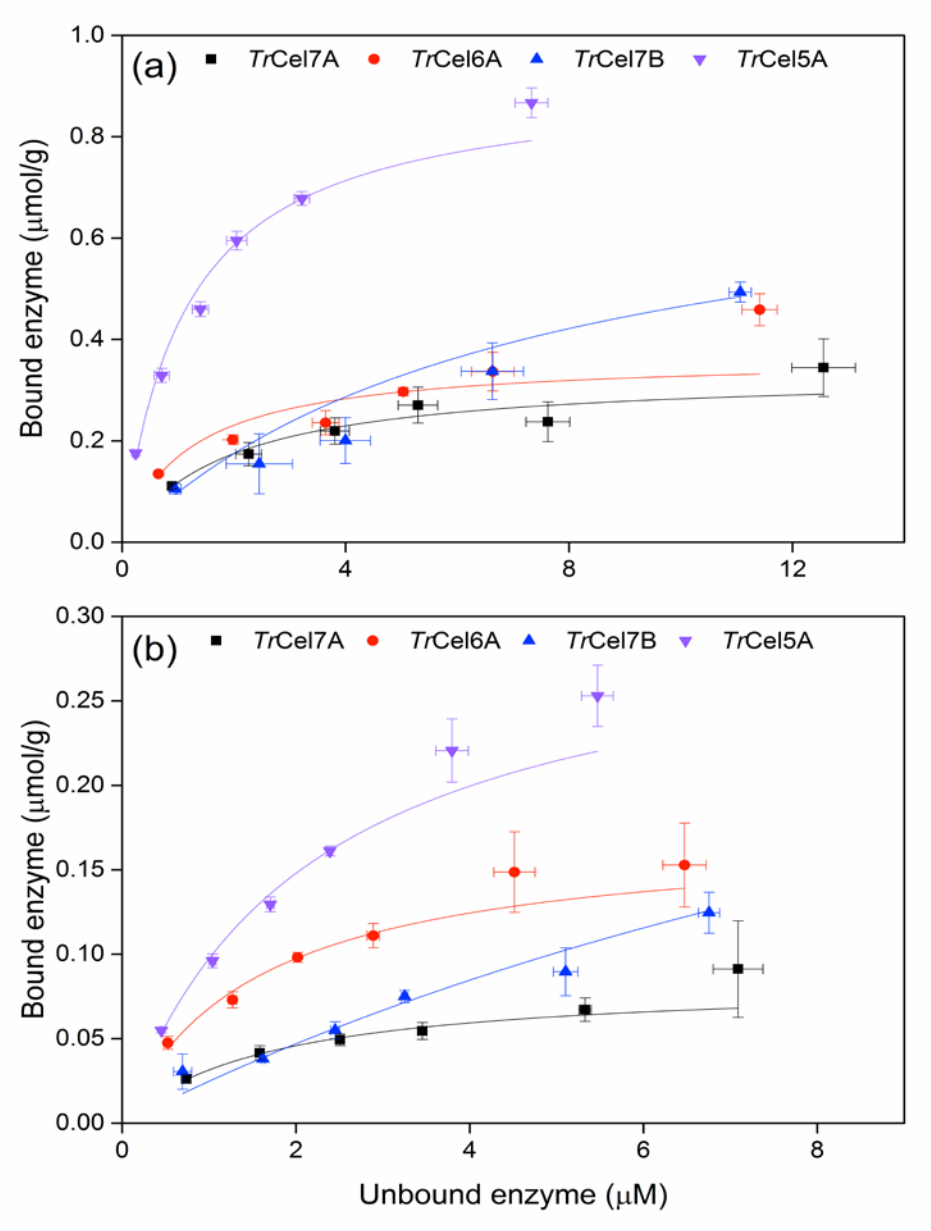

Figure 2. Adsorption of monocomponent cellulases to lignin-rich residues isolated from hydrothermally pretreated spruce (L-HPS) and hydrothermally pretreated wheat straw (L-HPWS) at initial protein concentration of 2 μM after 1 h at 45°C. Different letters indicate significant statistical difference based on ANOVA ($p \leq 0.05$). Data points and error bars respectively represent average and standard deviation from three experimental replicates.

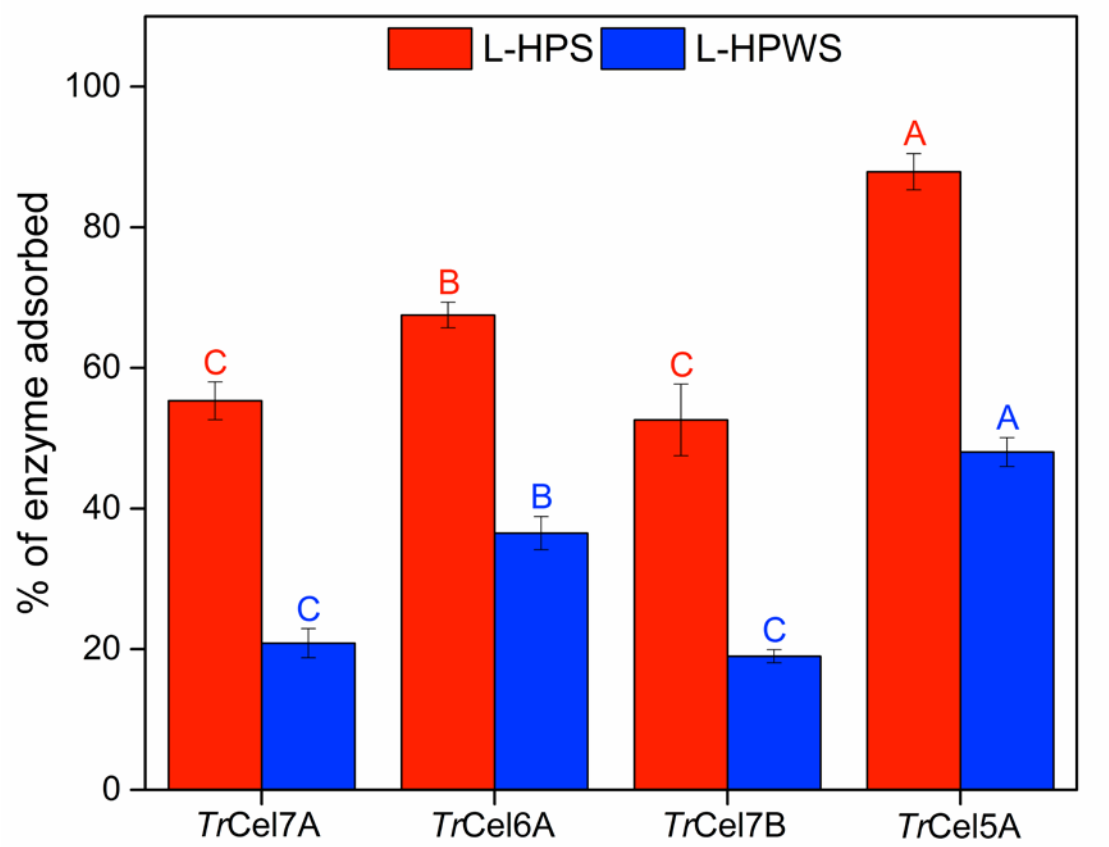

Figure 3. Response surface graphs displaying the fitting of experimental data of *Tr*Cel6A adsorption on lignin-rich residues isolated from hydrothermally pretreated spruce (L-HPS) (a & b) and hydrothermally pretreated wheat straw (L-HPWS) (c-f) modelled as reversible adsorption (a-d) and using Model 1 (e & f) with early (a, c & e) and late dilution (b, d & f).

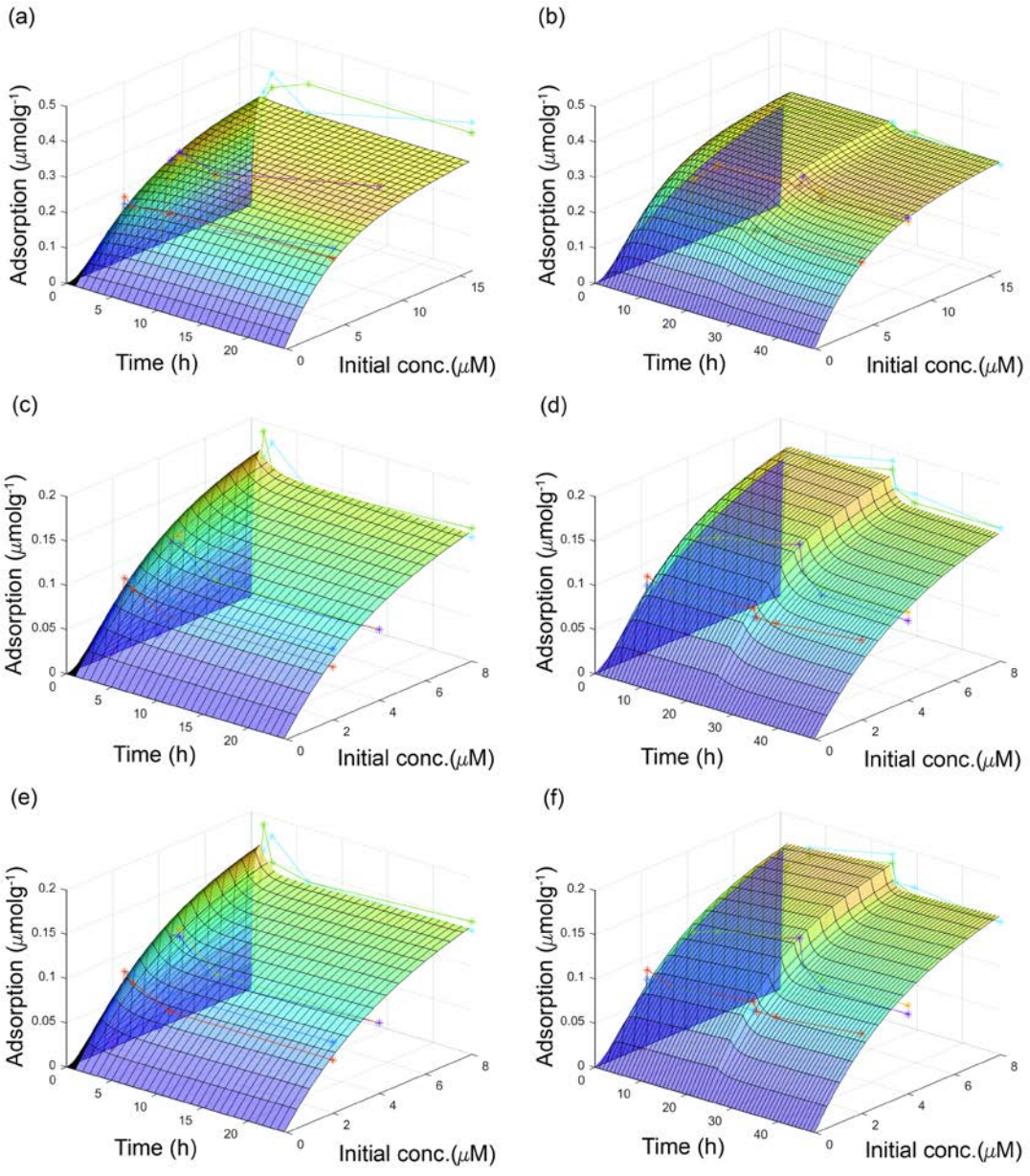

Figure 4. Competitive binding isotherms of *Tr*Cel6A and *Tr*Cel5A on lignin-rich residues isolated from hydrothermally pretreated (a) spruce (L-HPS) and (b) wheat straw (L-HPWS) at 45°C, pH 5.0 after 1 h. The tritium symbol ([^{3}H]) indicates radiolabeled enzyme. Solid lines represent fitting of the Langmuir adsorption model for one binding-site to the isotherms. Data points and error bars respectively represent average and standard deviation from three experimental replicates.

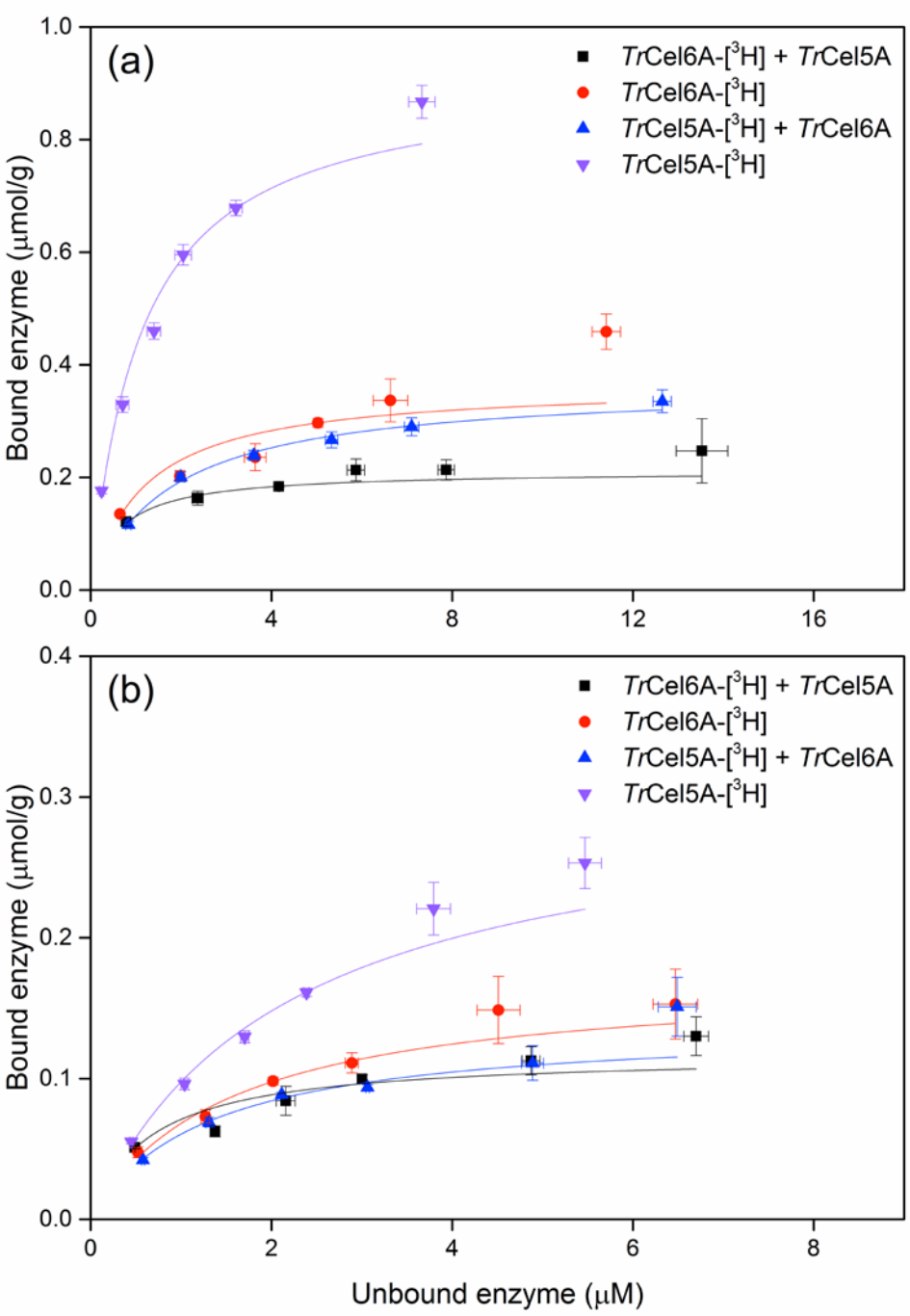

Table I. Summary of the characteristics of monocomponent cellulases used in this study

Enzymes	Old name	EC number	Domain architecture	M_W (kDa)[1]	pI[2]	Hydrophobic patch score[2]			Activity[3]
						Core	CBM	Total	
*Tr*Cel7A	CBHI	3.2.1.91	GH7-CBM1	56.0	3.6-4.3	6.7	6.6	13.3	5.7%
*Tr*Cel6A	CBHII	3.2.1.91	GH6-CBM1	56.7	5.4-6.2	14.1	1.9	16.0	14.8%
*Tr*Cel7B	EGI	3.2.1.4	GH7-CBM1	51.9	4.5-4.9, 4.7	6.2	0.8	7.0	378.2 nkat/mg
*Tr*Cel5A	EGII	3.2.1.4	GH5-CBM1	48.2	5.6	2.6	7.0	9.6	568.4 nkat/mg

1: Based on (Várnai et al., 2013).

2: Based on (Kellock et al., 2017); major isoform in pI measurement is underlined.

3: Activity of *Tr*Cel7A and *Tr*Cel6A is displayed as degree of RAC hydrolysis, whereas that of *Tr*Cel7B and *Tr*Cel5A is displayed as specific activity.

Table II. Langmuir isotherm parameters from the fitted adsorption data of monocomponent cellulases on isolated lignin-rich residues, L-HPS and L-HPWS, respectively

Adsorbent	Enzyme	$10 \times B_{max}$ (μmol/g)	$10 \times K_{ads}$ (l/μmol)	$10 \times \alpha$ (l/g)	R^2
L-HPS	*Tr*Cel7A	3.34 ± 0.28	5.48 ± 0.82	1.83 ± 0.31	0.957
	*Tr*Cel6A	3.66 ± 0.33	8.58 ± 1.86	3.14 ± 0.74	0.926
	*Tr*Cel7B	7.94 ± 1.29	1.42 ± 0.47	1.13 ± 0.42	0.972
	*Tr*Cel5A	9.13 ± 0.61	8.94 ± 1.32	8.16 ± 1.32	0.984
L-HPWS	*Tr*Cel7A	0.84 ± 0.06	6.02 ± 0.96	0.51 ± 0.09	0.975
	*Tr*Cel6A	1.72 ± 0.15	6.57 ± 1.28	1.13 ± 0.24	0.974
	*Tr*Cel7B	4.27 ± 1.64	0.62 ± 0.28	0.26 ± 0.16	0.967
	*Tr*Cel5A	3.07 ± 0.24	4.66 ± 0.61	1.43 ± 0.22	0.991

B_{max}: maximum adsorption capacity; K_{ads}: Langmuir adsorption constant; α: relative association constant ($B_{max} \times K_{ads}$). The reported constants and errors were obtained from fitting of three experimental replicates using the one binding-site Langmuir adsorption model.

Table III. The values and identifiability of fitting parameters of kinetic modelling

				Parameters				
LRRs	**Enzyme**	**Model**	**Fit R^2**	**k_{Rev}** $l^2/(\mu mol\ g\ h)$	**k_{-Rev}** $l/(g\ h)$	**k_{Ir}***	**B_{max}** $\mu mol/g$	**K_{ads}** $l/\mu mol$
HPS	*Tr*Cel6A	Model 1	0.896	0.0157	0.0163	3.82E-10	0.356	0.959
HPS	*Tr*Cel6A	Model 2	0.896	0.0120	0.0166	3.64E-03	0.357	0.723
HPS	*Tr*Cel6A	Reversible	0.896	0.0157	0.0164		0.356	0.957
HPS	*Tr*Cel6A	Irreversible	0.772			0.0217	0.272	
HPS	*Tr*Cel5A	Model 1	0.923	0.0165	0.0171	1.45E-07	0.562	0.962
HPS	*Tr*Cel5A	Model 2	0.923	0.0154	0.0167	7.81E-04	0.562	0.921
HPS	*Tr*Cel5A	Reversible	0.923	0.0160	0.0167		0.562	0.958
HPS	*Tr*Cel5A	Irreversible	0.784			0.0158	0.471	
HPWS	*Tr*Cel6A	Model 1	0.945	0.0397	0.0855	1.18E-03	0.223	0.464

HPWS	*Tr*Cel6A	Model 2	0.936	0.0311	0.0515	3.01E-04	0.217	0.603
HPWS	*Tr*Cel6A	Reversible	0.936	0.0314	0.0518		0.217	0.606
HPWS	*Tr*Cel6A	Irreversible	0.640			0.0743	0.124	
HPWS	*Tr*Cel5A	Model 1	0.967	0.0202	0.0626	4.05E-04	0.385	0.322
HPWS	*Tr*Cel5A	Model 2	0.965	0.0140	0.0512	4.49E-03	0.378	0.274
HPWS	*Tr*Cel5A	Reversible	0.965	0.0188	0.0525		0.379	0.357
HPWS	*Tr*Cel5A	Irreversible	0.570			0.0332	0.170	

LRRs	**Enzyme**	**Model**	**Fit**	**Identifiability (RSD at optimum fit)**			
			R^2	**k_{Rev}**	**k_{-Rev}**	**k_{Ir}**	**B_{max}**
HPS	*Tr*Cel6A	Model 1	0.896	9%	9%	4.86E+07%	3%
HPS	*Tr*Cel6A	Model 2	0.896	46%	10%	140%	3%
HPS	*Tr*Cel6A	Reversible	0.896	4%	10%		3%
HPS	*Tr*Cel6A	Irreversible	0.772			9%	1%
HPS	*Tr*Cel5A	Model 1	0.923	19%	23%	2.35E+05%	4%

HPS	*Tr*Cel5A	Model 2	0.923	28%	11%	513%	4%
HPS	*Tr*Cel5A	Reversible	0.923	10%	10%		5%
HPS	*Tr*Cel5A	Irreversible	0.784			0%	0%
HPWS	*Tr*Cel6A	Model 1	0.945	71%	65%	9%	4%
HPWS	*Tr*Cel6A	Model 2	0.936	30%	8%	3.03E+03%	3%
HPWS	*Tr*Cel6A	Reversible	0.936	3%	10%		4%
HPWS	*Tr*Cel6A	Irreversible	0.640			31%	3%
HPWS	*Tr*Cel5A	Model 1	0.967	78%	71%	49%	10%
HPWS	*Tr*Cel5A	Model 2	0.965	55%	10%	159%	13%
HPWS	*Tr*Cel5A	Reversible	0.965	25%	8%		13%
HPWS	*Tr*Cel5A	Irreversible	0.570			0%	0%

*) k_{Ir} is a 1st order rate constant with the unit l/(g h) in Model 1 and a 2nd order rate constant with the unit l^2/(µmol g h) in other models.

Table IV. Langmuir isotherm parameters from the fitted adsorption data of competitive binding of *Tr*Cel6A and *Tr*Cel5A on isolated lignin-rich residues

Adsorbent	Enzyme	$10 \times B_{max}$ (μmol/g)	$10 \times K_{ads}$ (l/μmol)	$10 \times \alpha$ (l/g)	R^2
L-HPS	*Tr*Cel6A-[^{3}H]	3.66 ± 0.33	8.58 ± 1.86	3.14 ± 0.74	0.926
	*Tr*Cel6A-[^{3}H] + *Tr*Cel5A	2.11 ± 0.05	16.3 ± 2.87	3.43 ± 0.61	0.948
	*Tr*Cel5A-[^{3}H]	9.13 ± 0.61	8.94 ± 1.32	8.16 ± 1.32	0.984
	*Tr*Cel5A-[^{3}H] + *Tr*Cel6A	3.64 ± 0.12	5.66 ± 0.45	2.06 ± 0.18	0.992
L-HPWS	*Tr*Cel6A-[^{3}H]	1.72 ± 0.15	6.57 ± 1.28	1.13 ± 0.24	0.974
	*Tr*Cel6A-[^{3}H] + *Tr*Cel5A	1.17 ± 0.11	15.4 ± 3.17	1.80 ± 0.41	0.898
	*Tr*Cel5A-[^{3}H]	3.07 ± 0.24	4.66 ± 0.61	1.43 ± 0.22	0.991
	*Tr*Cel5A-[^{3}H] + *Tr*Cel6A	1.38 ± 0.09	7.79 ± 1.29	1.08 ± 0.19	0.979

B_{max}: maximum adsorption capacity; K_{ads}: Langmuir adsorption constant; α: relative association constant ($B_{max} \times K_{ads}$). The reported constants and errors were obtained from fitting of three experimental replicates using one binding-site Langmuir adsorption model.